Journal of Engineering Science and Technology
Vol. 10, No. 2 (2015) 224 - 234

COMPARATIVE ANALYSIS OF QUANTUM EFFECTS IN NANO-SCALE MULTIGATE MOSFETS USING VARIATIONAL APPROACH

V. PALANICHAMY[1,*], N.B. BALAMURUGAN[2]

[1]Department of Electronics and Communication Engineering,
Dayananda Sagar College of Engineering, Bangalore, India
[2]Department of Electronics and Communication Engineering, Thiagarajar
College of engineering, Madurai, Tamilnadu, India
*Corresponding Author: ervimala@gmail.com

Abstract

In this work, the performance of multiple-gate SOI MOSFETs is analysed using variational approach including quantum effects. An analytical model is derived to accounting the quantum effects at the silicon (Si)/silicon dioxide (SiO_2) interface. A general procedure is used for calculating the quantum inversion charge density. Using this inversion charge density, the drain current is obtained. Our model results are compared with the simulation results and its shows very good agreement. Our results highlighted that cylindrical surrounding gate MOSFET is a good candidate to obtain the high drain current compared with other two devices.

Keywords: Multiple gate MOSFETs, Quantum effects, Centroid, Inversion charge density, Drain current.

1. Introduction

To extend CMOS scaling down to 10 nm gate length and beyond [1], multiple-gate MOSFETs have been intensively studied because of their better short channel characteristics [2] and higher current. The term multiple-gate refers to a field-effect transistor with the gate electrode warped around several sides of the device. Among the different multiple gate structures proposed, Double-gate, Tri-gate and Surrounding-gate MOSFETs are accepted widely among device engineers. The scaling of Multiple-Gate MOSFET requires the use of an increasingly thinner Silicon film, for which new phenomena have to be taken into account, such as quantum-mechanical effects. These phenomena induce a strong subband splitting and the carrier confinement in the narrow potential well formed by the Si/SiO_2

Nomenclatures

C_G	Gate capacitance
$\hbar$	Reduced Planck constant
I_d	Drain current, mA
L	Channel length, nm
m_o	Electron rest mass
N_A	Accepter concentration
N_{inv}	Inversion charge areal density
Q_d	Depletion charge density
R	Radius of the Silicon pillar region, nm
r	Radial direction
t_{ox}	Oxide thickness, nm
t_{si} ,H	Silicon thickness, nm
V_{ds}	Drain source voltage, V
V_{gs}	Gate source voltage, V
V_{ox}	Oxide potential
V_t	Thermal voltage
W	Silicon width, nm

Greek Symbols

ε_{ox}	Oxide permittivity
ε_{si}	Silicon permittivity
ϕ	Potential
ϕ_F	Bulk potential
ϕ_s	Semiconductor work function
μ	Mobility
ψ	Wave function of the particle

interface [3]. Quantum effects sensibly modify the three dimensional (3-D) carrier distributions in the channel, the most important effect being the shift of the charge centroid away from the interfaces into the Silicon film. The inversion charge and the drain current are reduced in the quantum case with respect to the "classical" case (i.e., without quantum effects). Quantum-mechanical confinement is stronger when the silicon film is thinner. It has been shown that the energy quantisation becomes important for channels below 10 nm thick, for which it becomes mandatory to take into account quantum effects in the device simulation [4].

Few works are addressing the quantum effects through multigate structures via the simulation and numerical approaches [5, 6]. Nevertheless, there is only one analytical modeling of multigate quantum effects [7], which has more computational complexity. The variational approach holds good to couple the Schrodinger and Poisson equations and could well predict the carrier density reduction due to quantum effects of multigate structures. The extracted inversion charge density is used to evaluate drain current voltage (I-V) characteristic of the device for quantum mechanical approach. The purpose of this paper is to analyse the performance of multigate MOSFETs including quantum effects using variational approach.

2. Model Formulation and Parameters Computations

MOS inversion layer carrier density and the drain current are key parameters for MOSFET characterisation and modelling. To avoid the computational complexity of the fully self consistent solution of Schrodinger and Poisson equations, in an inverted MOS structure, an alternative is to use an approximate treatment that takes into account the quantisation effect occurring at the Si/SiO_2 interface. In this section we briefly explain the general algorithm implemented in our model to obtain I – V characteristics of the transistor. Figure 1 shows the different intrinsic schematic diagrams of multigate SOI MOSFETs (Double-gate, Tri-gate and Surrounding-gate) have been examined.

Figure 2 shows the flowcharts where we represent two procedures labelled Figs. 2(a) and (b) respectively used to: (a) steps for variational approach and (b) evaluate the device characteristics. To model quantum effects, the method used in this paper refers to the variational approach which involves an analytical solution of the ground state energy based itself initially on the choice of trial wave function. It is essential to study the wave function, and can be determined by solving the Poisson and Schrodinger equations. The optimum trial wave functions (ψ_o) for Double-gate (DG) [8], Tri-gate (TG) [9] and Surrounding gate (SG) [10] MOSFETs given in Table 1, where, t_{si} is the silicon film thickness of DG MOSFET. H and W are silicon film thickness and width of TG MOSFET. R is the radius of silicon film SG MOSFET. a_o and b_o are the unknown parameters. Normalisation of the above wave function gives the expression for corresponding a_o in terms of b_o. Then we follow the variational approach given in Fig. 2(a) to solve the coupled Poisson and Schrodinger equations.

Table 1. Trail wave functions used in our model.

Device	Trail wave function
DG	$\psi_0(x) = \left(a_0 \sqrt{\frac{2}{t_{si}}} \sin\left(\frac{\pi x}{t_{si}}\right) \left(e^{-b_0 x / t_{si}} + e^{-b_0 (t_{si}-x)/t_{si}}\right)\right)$
TG	$\psi_o(x,y) = \left(a_0 \sqrt{4/HW} \sin\left(\frac{\pi x}{H}\right) \left[\sin\left(\frac{\pi y}{W}\right)\right]^{1/2} \left(e^{-b_0 x/H}\right)\left(e^{-b_0 y/W} + e^{-b_0 (W-y)/W}\right)\right)$
SG	$\psi_0(x) = \left(a_0 \sqrt{\frac{1}{R}} \sin\left(\frac{\pi(x+R)}{2R}\right) \left(e^{-b_0 (x+R)/2R}\right)\right)$

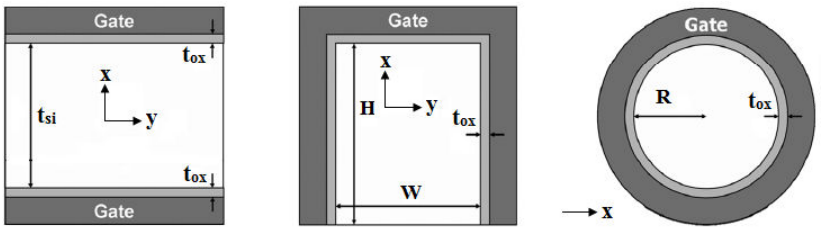

Fig. 1. Schematic diagrams of multigate MOSFET cross section.

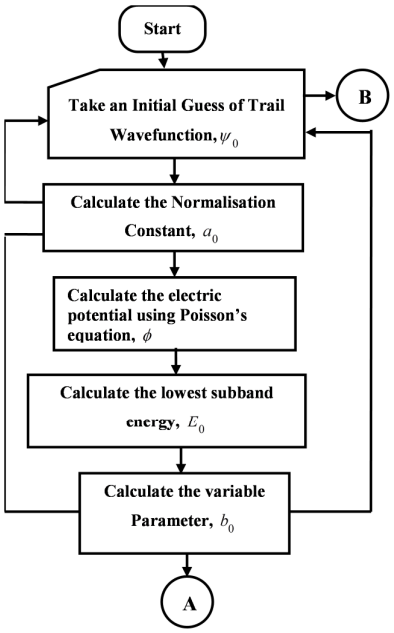

Fig. 2(a). Flowchart/algorithm for the variational approach including quantum effects.

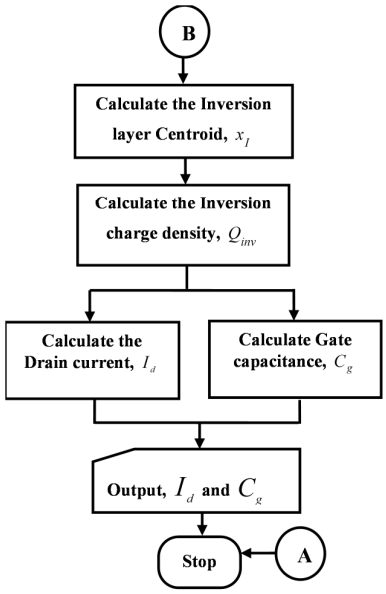

Fig. 2(b). Flowchart for the extraction of transfer characteristics and gate capacitance using trial wave function, ψ_o.

2.1. DG MOSFETs

Poisson equation is given as,

$$\frac{d^2}{dx^2}\phi(x) = \frac{q}{\varepsilon_{si}}(N_A + n(x)) \tag{1}$$

where q is the electronic charge, ε_{si} is the silicon permittivity, $\phi(x)$ is the electric potential in the silicon, $n(x)$ is the electron density and N_A is the accepter concentration.

To include the quantum effects, the relation between the $n(x)$ and the trial wave function $\psi_0(x)$ is given as,

$$|\psi_0(x)|^2 = \frac{n(x)}{N_{inv}} \tag{2}$$

Substituting Eq. (2) into Eq. (1), we can get,

$$\frac{d^2\phi(x)}{dx} = -\frac{q}{\varepsilon_{si}} N_{inv}|\psi_0(x)|^2 \tag{3}$$

The Schrodinger equation is written as,

$$-\frac{h^2}{8\pi^2 m_x}\frac{d^2}{dx^2}\psi_0(x)+(-q)\phi(x)\psi_0(x)=E_0\psi_0(x) \tag{4}$$

where, h is the Plank's constant, E_0 is the lowest subband energy, m_x is the effective mass of electrons. Now, solve the Schrodinger equation using $\phi(x)$ via variational approach to get the lowest subband energy E_0 . b_0 is evaluated by $dE_0/db_0=0$. With the approximation b_0 is derived as,

$$b_0 \approx t_{si}\left(\frac{qm_x\pi^2(Q_d+\frac{5}{6}Q_{inv})}{\varepsilon_{si}h^2}\right)^{1/3} \tag{5}$$

The inversion charge density was calculated by the determination of inversion layer centroid. The inversion layer centroid (x_1) is obtained as,

$$x_1 = 2\int_0^{t_{si}/2} x[\psi_o(x)]^2\,dx \tag{6}$$

The inversion charge density can be related to the gate voltage as follows,

$$Q_{inv}=2C_{ox}{}^{1}\left[V_{gs}-V_t\right] \tag{7}$$

where,

$$C_{ox}{}^{1}=\frac{C_{ox}}{1+C_{ox}\frac{x_1}{\varepsilon_{si}}} \tag{8}$$

$$V_t=\phi_{ms}+\varphi_{dep}+\frac{Q_d}{C_{ox}} \tag{9}$$

φ_{dep} is the depletion potential, C_{ox} is the gate oxide capacitance, x_1 is the inversion layer centroid, ϕ_{ms} is the work function difference between gate and silicon film, and V_t is a constant threshold voltage for strong inversion. The drain current in DG MOSFET is expressed as,

$$I_{d,DG}=\mu\frac{W}{L}\int_0^{V_{ds}} Q_{inv}\,dV \tag{10}$$

2.2. TG MOSFETs

The Poisson equation for the trigate MOSFETs is given as,

$$\frac{d^2\phi(x,y)}{dxdy}=\frac{-q}{\varepsilon_{si}}n(x,y) \tag{11}$$

Using the relation in (2), we get the Poisson equation in terms of trial wave function as,

$$\frac{d^2\phi(x,y)}{dxdy} = -\frac{q}{\varepsilon_{si}} N_{inv} \left|\psi_0(x,y)\right|^2 \tag{12}$$

The Schrodinger equation is written as,

$$\frac{-h^2}{2m_x}\frac{d^2\psi_0(x,y)}{dxdy} + (-q)\phi(x,y)\psi_0(x,y) = E_0\psi_0(x,y) \tag{13}$$

Based on quantum mechanical variational approach the b_0 is derived as,

$$b_0 \approx (W+H)\pi^2\left(\frac{5}{12}\frac{qm_x Q_{inv}}{\varepsilon_{si}h^2}\right) \tag{14}$$

The centroid x_1 is obtained as,

$$x_1 = 3\int_0^W\int_0^H xy\,\psi_0(x,y)dxdy \tag{15}$$

The inversion charge density, Q_{inv} for TG MOSFET can be obtained by using Eqs. (7)-(9). The drain current in trigate MOSFET is expressed as

$$I_{d,TG} = \mu\pi\left(\frac{H+W}{L}\right)\int_0^{V_{ds}} Q_{inv}\,dV \tag{16}$$

2.3. SG MOSFETs

The Poisson equation is given as,

$$\frac{d^2\phi(x)}{dx^2} + \frac{1}{x}\frac{d\phi(x)}{dx} = \frac{q}{\varepsilon_{si}} n(x) \tag{17}$$

The Poisson equation in terms of trial wave function is

$$\frac{d^2\phi(x)}{dx^2} + \frac{1}{x}\frac{d\phi(x)}{dx} = \frac{q}{\varepsilon_{si}} N_{inv}\left|\psi_0(x)\right|^2 \tag{18}$$

The Schrodinger equation is written as,

$$\frac{-h^2}{2m_x}\frac{d^2\psi_0(x)}{dx^2} + (-q)\phi(x)\psi_0(x) = E_0\psi_0(x) \tag{19}$$

Based on quantum mechanical variational approach the b_0 is derived as,

$$b_o \approx R\pi^2\left(\frac{5}{6}\frac{qm_x Q_{inv}}{\varepsilon_{si}h^2}\right) \tag{20}$$

The centroid x_1 is obtained as,

$$x_1 = \int_0^R r\,\psi_0^{\,2}\,dr \tag{21}$$

Since it's a cylindrical shape we can't use the Q_{inv} model present in Eqs. (7)-(9). The inversion charge density, Q_{inv} for SG MOSFET can be obtained based on [11] using the modelled centroid. The drain current in SG MOSFET is expressed as,

$$I_{d,SG} = \mu \frac{2\pi R}{L} \int_0^{V_{ds}} Q_{inv}(V) dV \tag{22}$$

3. Results and Discussion

The comparison results of our inversion charge based analytical model for multigate devices are presented in this section. For the comparison purpose, the silicon film thickness is taken as a common parameter. Table 2 gives the symbols used to represent silicon film thickness for the various kinds of multigate MOSFETs. Calculations are performed using n-channel devices with metal (Al with $\varphi_m = 4.10ev$) gates, oxide thickness t_{ox} at room temperature (300°) and values of various parameters for multigate MOSFETs.

Table 2. Silicon thickness for various multigate MOSFETs.

Device	Silicon thickness (t_{si}=)
DG	t_{si}
TG	H
SG	$2R$

The accuracy of the proposed model is verified using the commercially available TCAD Sentaurus device simulator. Sentaurus Device implements four different quantisation models, such as Van Dort model, 1D Schrödinger equation model, Density gradient model and Modified local-density approximation (MLDA) model. In our work the 1D Schrödinger equation model is used to evaluate the influence of quantisation effects."The accuracy of the proposed model is verified using the commercially available TCAD Sentaurus device simulator. Sentaurus Device implements four different quantisation models, such as Van Dort model, 1D Schrödinger equation model, Density gradient model and Modified local-density approximation (MLDA) model. In our work the 1D Schrödinger equation model is used to evaluate the influence of quantisation effects.

The calculated energies of the present model shown in Fig. 3 are in good agreement with simulation results. Figure 3 shows the variation of the minimum energy of the first subband (E_o) as a function of electron concentration with different gate configurations. The energy of the lowest subband decreases, when the effective gate numbers is increased and it increases when the average electron concentration increases. This is explained by many body electron–electron interactions: as the concentration of electron increases, the local electron charge increases and the repulsive force between these electrons increases. More energy is thus required to further increase the electron concentration and, as a result, the energy of the subbands increases. The most interesting parameter that can be modelled is the average inversion layer penetration (defined as the inversion

charge centroid), which has been used to quantify the influence of quantum effects on the inversion charge of MOS devices.

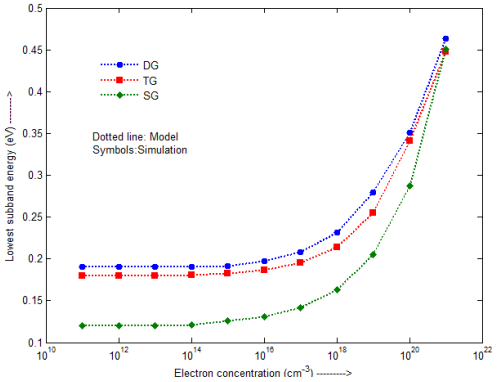

Fig. 3. Lowest subband energy as a function of electron concentration for different gate configurations with t_{si} = 5 nm.

We calculated the inversion charge centroid making use of our model the results versus inversion charge density (N_{inv}) are plotted in Fig. 4. The centroid shows the expected behaviour and it can be seen that its value decreases as the inversion charge increases since the charge distribution shifts toward the Si/SiO_2 interface. The model presented here exactly matches with simulation data's for different device structures. For high electron concentration the centroid value decreases considerably. This in turn suppresses the charge carriers near the drain side. The reduction of charge carrier population suppresses the hot electron effects, which is one of the Short Channel Effects (SCEs).

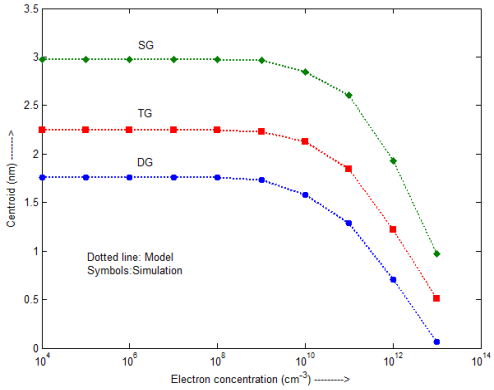

Fig. 4. Inversion charge centroid versus electron density for various device structures at room temperature.

Figure 5 shows the average inversion charge density versus silicon thickness for various device structures. The silicon thickness varies from 0 to 12 nm while keeping the gate voltage as constant (V_{gs}=0.5V). Clearly we can observe that the

average electron concentration needed to reach the threshold voltage increases as device dimensions are reduced. The inversion charge density of SG is high compare to that of the other transistors.

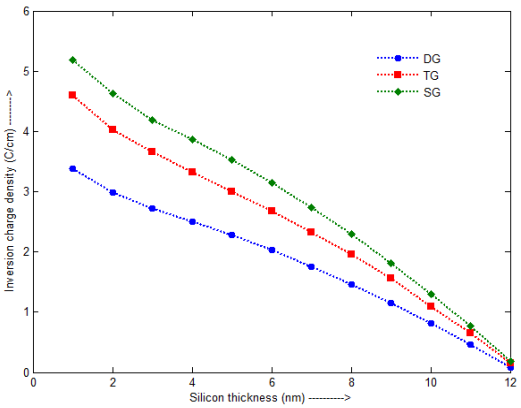

Fig. 5. Inversion charge density as a function of silicon film thickness. The simulation results obtained, including quantisation, are plotted in symbols. The data obtained making use of the model is plotted in dotted lines.

Figure 6 shows the drain current versus drain voltage for multigate MOSFETs with V_{gs}= 1V and t_{si} = 5 nm. From the figure, It can be observed that the drain current increase with increasing drain voltage. The drain current increases linearly as device gate numbers are increased. Very good agreement is obtained between the simulation and the analytical model. The drain current I_{ds} in the SG is much higher than other transistor characteristics. In surrounding gate architecture, the gate completely controls the channel in all the sides. The influence of gate control by gate voltage over the channel is more compared to high drain voltage. Hence high drain current does not affect channel, which invariably suppresses the Drain Induced Barrier Lowering (DIBL) effects.

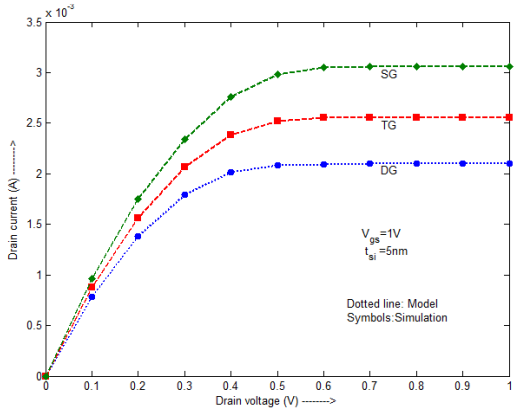

Fig. 6. I-V Characteristics of multigate MOSFETs with 5 nm silicon thickness and the gate source voltage is 1V. Dashed line: Modelled data's. Symbols: Simulation data's.

Figure 7 shows the threshold voltage as a function of device dimension for different gate configurations. The threshold voltage is defined as a gate voltage at which the derivative of the transconductance, reaches a maximum. As expected, the threshold voltage increases when the device thickness is reduced. However, that increase of VTH is reduced when the effective number of gates is increased. This can be explained by the decrease of inversion electron concentration needed to reach VTH (Fig. 5) and by a decrease of the energy of the lowest subband (Fig. 3) when the effective number of gates is increased.

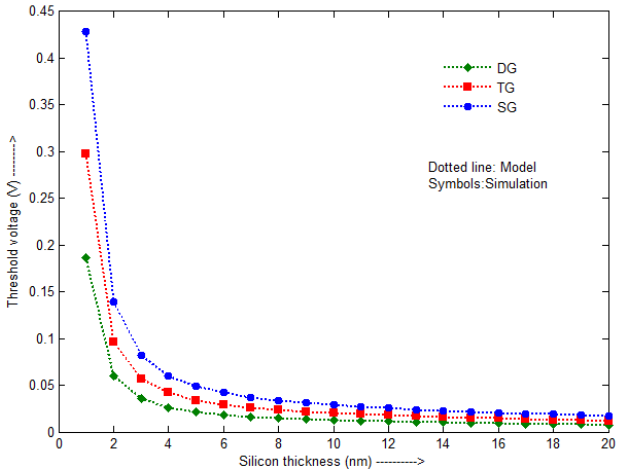

Fig. 7. Threshold voltage of multigate MOSFETs as a function of silicon thickness. Dashed line: Modelled data's. Symbols: Simulation data's.

4. Conclusions

A unified strategy for compact energy quantisation modeling of various forms of double-gate, tri-gate and surrounding gate MOSFETs has been presented. It is based on the closed-form analytical solutions of Poisson and Schrodinger equations using variational approach. We have investigated in detail the lowest subband energy, centroid, inversion charge density and drain current of the three types of MOSFETs. Obviously the cylindrical surrounding gate MOSFETs has more advantage compare to the other types of devices. A newly developed compact model for cylindrical surrounding gate MOSFETs can be implemented in SPICE simulator for efficient circuit simulation. This method is cost effective, when compare with commercially available multi-dimensional quantum solver.

Acknowledgments

The authors are grateful to the Women Scientist Scheme-A (WOS-A), Department of Science and Technology (DST), Government of India, India for providing the necessary financial assistance to carry out this research work.

References

1. International technology roadmap for semiconductors (2013). Retrieved May 20, 2013 from http://www.itrs.net.
2. Colinge, J.P. (2004). Multiple-gate SOI MOSFETs. *Solid State Electronics,* 48(6), 894-905.
3. Taur, Y.; and Ning, T.H. (1998). *Fundamentals of modern VLSI Devices*. Cambridge University Press.
4. Bescond, M.; Nehari, K.; Autran, J.L.; Cavassilas, N.; Munteanu, D.; and Lannoo, M. (2004). 3D quantum-modelling and simulation of multi-gate nanowire MOSFETs. *IEEE International Electron Devices Meeting, IEDM Technical Digest*, 617-620.
5. Godoy, A.; Ruiz-Gallardo, A.; Sampedro, C.; and Gámiz, F. (2007). Quantum-mechanical effects in multiple-gate MOSFETs. *Journal of Computational Electronics*, 6(1-3), 145-148.
6. Yun, S.R.N.; Chong, G.Y.; Jong, T.P.; and Jean, P.C. (2008). Quantum-mechanical effects in nanometer scale MuGFETs. *Microelectronic Engineering*, 85(8), 1717-1722.
7. Song, J.Y.; Bo, Y.; Yu, Y.; and Yuan, T. (2009). A review on compact modelling of multiple-gate MOSFETs. *IEEE Transactions on Circuits and Systems*, 56(2), 1858-1869.
8. Vimala, P.; and Balamurugan, N.B. (2013). Modelling the centroid and inversion charge density in double-gate MOSFETs including quantum effects. *International Journal of Electronics,* 100(9), 1283-1295.
9. Vimala, P.; and Balamurugan, N.B. (2013). Modelling and simulation of centroid and inversion charge density in cylindrical surrounding gate MOSFETs including quantum effects. *Journal of Semiconductors,* 34(11), 1-6.
10. Vimala, P.; and Balamurugan, N.B. (2014). Modeling and simulation of nanoscale Tri-gate MOSFETs including quantum effects. *Journal of Semiconductors*, 35(2), article in press.
11. Roldan, J.B.; Andres Godoy.; Francisco, G.; and Balaguer, M. (2008). Modelling the centroid and the inversion charge in cylindrical surrounding gate MOSFETs, *IEEE Transactions on Electron Device*, 55(1), 411-416.